

Resonant excitation cross-sections of erbium in freestanding GaN bulk crystals

Z. Y. Sun, Y. Q. Yan, W. P. Zhao, J. Li, J. Y. Lin, and H. X. Jiang^{a)}

Department of Electrical and Computer Engineering, Texas Tech University, Lubbock, Texas 79409, USA

(Received 20 March 2018; accepted 4 May 2018; published online 17 May 2018)

Erbium doped GaN (Er:GaN) is a promising candidate as a new gain medium for high energy lasers. The excitation and emission mechanisms as well as the transition cross sections of the pump and laser wavelength are of paramount importance for understanding the performance of lasers and amplifiers made of Er:GaN materials. We report here the results of direct measurements of resonantly excited photoluminescence emission, photoluminescence excitation, and optical absorption spectroscopy in the 1.5 μm “retina-safe” spectral region performed on freestanding Er:GaN bulk crystals synthesized by hydride vapor phase epitaxy. The results established that 1514 nm and 1538 nm are the most appropriate resonant pump wavelengths for achieving gain and lasing, which differs from Er in YAG and glass hosts. The absorption coefficients (α) and absorption cross-sections (σ_{exc}) of Er in GaN in the 1.5 μm window have been directly measured, providing $\sigma_{\text{exc}} = 1.4 \times 10^{-20} \text{ cm}^2$ and $2.7 \times 10^{-20} \text{ cm}^2$ for 1514 nm and 1538 nm pump wavelengths, respectively. These values are considerably higher than those of Er ions in glass and YAG hosts. *Published by AIP Publishing.*

<https://doi.org/10.1063/1.5030347>

Solid-state high energy lasers (HELs) operating in the “retina-safe” spectral region have attracted a great attention and are highly sought-after for use in defense, industrial processing, communications, medicine, spectroscopy, imaging, and various other applications where the laser is expected to travel long distances in free space.¹ At the heart of a high energy laser (HEL) system is its optical gain medium. Currently, one of the dominant gain media for HELs is neodymium doped YAG (Nd:YAG), emitting at 1.06 μm . When doped in a host, the emission lines resulting from the intra-4f transitions from the first excited state manifold ($^4I_{13/2}$) to the ground state manifold ($^4I_{15/2}$) in Er^{3+} ions are near 1.5 μm , a wavelength window providing a better “retina-safety” as well as atmospheric transmittance than the wavelengths below or close to 1 μm .^{2,3} Several groups have investigated and demonstrated highly promising results for Er doped YAG (Er:YAG) gain medium.^{4–10} Nevertheless, finding gain materials operating in the 1.5 μm window with improved thermal properties over YAG is highly desirable for future emerging HEL applications.

Er doped GaN (Er:GaN) is a promising candidate as a gain medium for HELs. GaN has a much higher thermal conductivity of $\kappa = 253 \text{ W/mK}$ (versus 14 W/mK for YAG),¹¹ a smaller thermal expansion coefficient of $\alpha \approx 3.53 \times 10^{-6} \text{ }^\circ\text{C}^{-1}$ (versus $8 \times 10^{-6} \text{ }^\circ\text{C}^{-1}$ for YAG),¹¹ and smaller temperature coefficient of the refractive index, $dn/dT = 0.7 \times 10^{-5} \text{ }^\circ\text{C}^{-1}$ (versus $1.75 \times 10^{-5} \text{ }^\circ\text{C}^{-1}$ for YAG).¹² The thermal shock parameter, κ/α^2 , which is a rough measure of the maximal attainable lasing power for a typical solid-state laser attached to a heat sink,^{13,14} indicates that GaN host has the potential to outperform YAG host by nearly 2 orders of magnitude in terms of maximal lasing power. With a smaller dn/dT , GaN HELs potentially provide a better beam quality than those with YAG host for the same temperature variance across the gain medium. Moreover, prior results have demonstrated that

1.5 μm Er emission in GaN have a high temperature stability due to the wide bandgap nature of GaN.^{15–17}

To realize practical design of gain materials for HEL, thick layers of Er:GaN are needed to provide adequate dimensions to support a sufficient pumping light absorption and surface area for heat removal as well as mechanical strength. On the other hand, the excitation and emission mechanisms as well as the transition cross sections of the pump and laser wavelengths are of paramount importance for understanding the performance of lasers and amplifiers made of Er:GaN materials. Due to the lack of thick Er:GaN crystals in the past, most of the previous spectroscopic studies of Er:GaN were conducted on thin epilayers with a thickness of a few microns produced by metal organic chemical vapor deposition (MOCVD) or molecular beam epitaxy.^{17–28} Consequently, it was not possible to directly measure the optical absorption spectra and hence the optical absorption cross sections for Er ions in GaN in the 1.5 μm window in the past. The optical absorption cross sections of Er in GaN at selective wavelengths were indirectly deduced from the flux saturation method via the measurements of PL emission intensity as a function of excitation photon flux together with emission lifetime²³ or from the emission spectra together with the use of McCumber’s theory.²⁶ In this work, we performed resonantly excited photoluminescence (PL) emission, photoluminescence excitation (PLE) and optical absorption spectroscopy measurements in the 1.5 μm spectral region on thick freestanding Er:GaN bulk crystals synthesized by hydride vapor phase epitaxy (HVPE), from which important parameters of optical absorption coefficients and cross-sections at the desired resonant pump wavelengths have been directly obtained.

Quasi-bulk Er:GaN crystals with a thickness around 1.2 mm were synthesized by hydride vapor phase epitaxy (HVPE), which is an established technique for producing GaN quasi-bulk crystals.²⁹ Freestanding Er:GaN crystals were obtained by using a laser-lift-off process as illustrated

^{a)}hx.jiang@ttu.edu

in Fig. 1. Prior to the deposition of Er:GaN, a 3 μm GaN epilayer serving as a template was grown on sapphire (0001) substrate by MOCVD. The GaN/sapphire template was then transported into an HVPE reactor, and a layer of Er:GaN with a thickness around 1.2 mm was synthesized at a temperature of 1030 $^{\circ}\text{C}$ at a growth rate of about 200 $\mu\text{m}/\text{h}$. After the HVPE growth, the sapphire substrate was removed by a laser-lift-off process.¹⁶ The obtained freestanding Er:GaN was then polished and cut into different geometries. The PL emission spectra were measured using a 980 nm laser diode as an excitation source, and a monochromator (SpectraPro-300i, Acton Research Corporation) in conjunction with an IR detector was used to disperse the PL signal. The PLE spectra were measured using a tunable semiconductor laser (TSL-550, Santec, with a spectral range of 1500–1630 nm and a full-width at half maximum of 0.3 pm) as an excitation source and the same monochromator/IR detector was used to record the PLE signal. The optical absorption spectra were measured using the same tunable semiconductor laser as the excitation source and an IR power meter (from Newport) as a detector.

Figure 2 shows a room temperature PL emission spectrum of a freestanding Er:GaN crystal under a 980 nm laser excitation, which resonantly excites carriers from the ground state manifold ($^4I_{15/2}$) to the upper $^4I_{11/2}$ manifold of Er^{3+} ions. The spectrum displays clearly resolved peaks, apparently resulting from the transitions between Stark sublevels of the first excited state ($^4I_{13/2}$) and ground state ($^4I_{15/2}$).²⁷ It should be emphasized that the PL spectrum exhibits no features below 1500 nm. This is different from the situations for Er ions in YAG and glass hosts, in which Er^{3+} ions exhibit a strong absorption/emission line at 1470 nm and 1480 nm, respectively, corresponding to a resonant transition between the bottom of the $^4I_{15/2}$ ground state manifold and the top of the $^4I_{13/2}$ first excited state manifold. In fact, this transition near 1470–1480 nm is one of the most common excitation lines employed to achieve optically pumped low quantum defect Er:YAG lasers^{4–10} and Er doped fiber lasers as well as optical amplifiers.³⁰

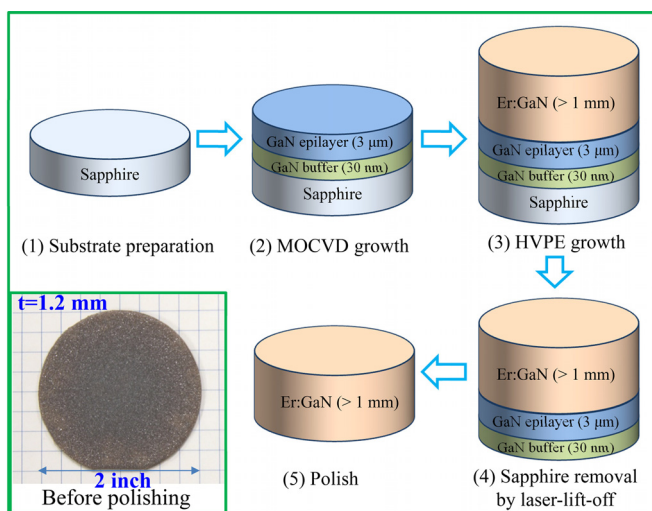


FIG. 1. Growth and processing procedures for obtaining freestanding Er:GaN bulk crystals. The inset is an image of an as grown 2-in. freestanding Er:GaN wafer with a thickness of 1.2 mm.

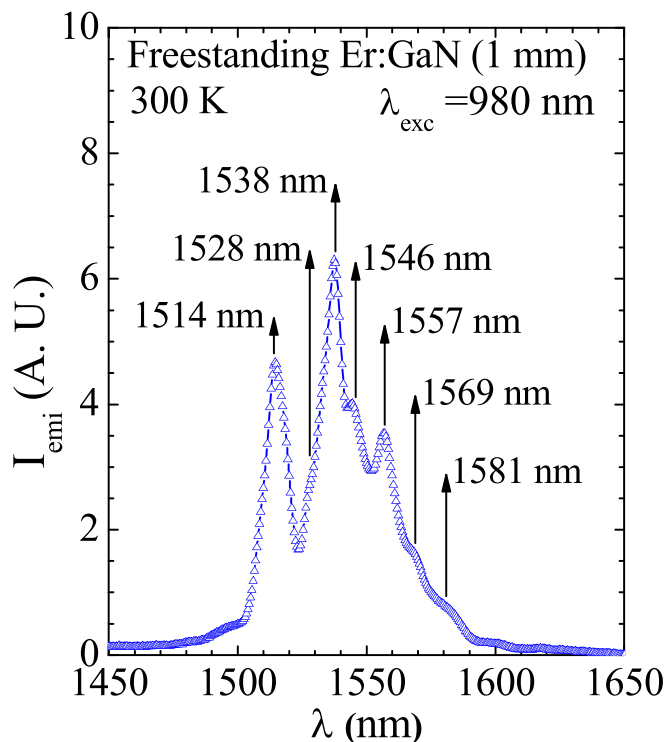


FIG. 2. Room temperature photoluminescence emission spectrum of a freestanding Er:GaN sample measured the 1.5 μm window, excited by a 980 nm laser.

Guided by the PL emission spectrum shown in Fig. 2,³¹ we have performed the room temperature PLE spectroscopy on a freestanding Er:GaN crystal covering the most relevant excitation wavelength range from 1500 nm to 1545 nm with the detection wavelength fixed at 1570 nm, aimed at establishing the most suitable pump wavelengths for the realization of future HELs based on Er:GaN bulk crystals. The PLE spectrum shown in Fig. 3 clearly revolves 2 dominant peaks at 1514 nm and 1538 nm in the measured excitation wavelength range. These two wavelengths correspond well with the two emission peaks observed at 1.514 μm and 1.538 μm in the PL emission spectrum shown in Fig. 2. To enable the optical absorption measurements, an Er:GaN sample with its Er^{3+} dopant concentration $N_{\text{Er}} = 3.0 \times 10^{19}$ ions/ cm^3 as calibrated by secondary ion mass spectrometry (SIMS) measurements was double side polished. Figure 4(a) is a plot of the optical absorption spectrum, which exhibits three main absorption peaks at 1514 nm, 1538 nm, and 1556 nm. These absorption peaks correspond well with the emission peaks observed in the PL emission spectrum shown in Fig. 2 as well as with the PLE spectrum shown in Fig. 3.

From the measured absorption coefficients (α), the excitation cross-sections (σ_{exc}) of Er in GaN can be directly calculated from the relation of $\sigma_{\text{exc}} = \alpha/N_{\text{Er}}$ and the results for the absorption cross-sections are displayed in Fig. 4(b). The results clearly indicate that in order to achieve lasing and amplification at 1.57 μm , the optimal pumping wavelength is either 1514 nm or 1538 nm, corresponding to a quasi-four-level and a quasi-three-level system, respectively. It is worth to point out that due to the lack of thick Er:GaN crystals and hence the inability for directly obtaining PLE and optical absorption spectra in the 1.5 μm window in the past, our outstanding of optical transitions in Er:GaN was guided by the

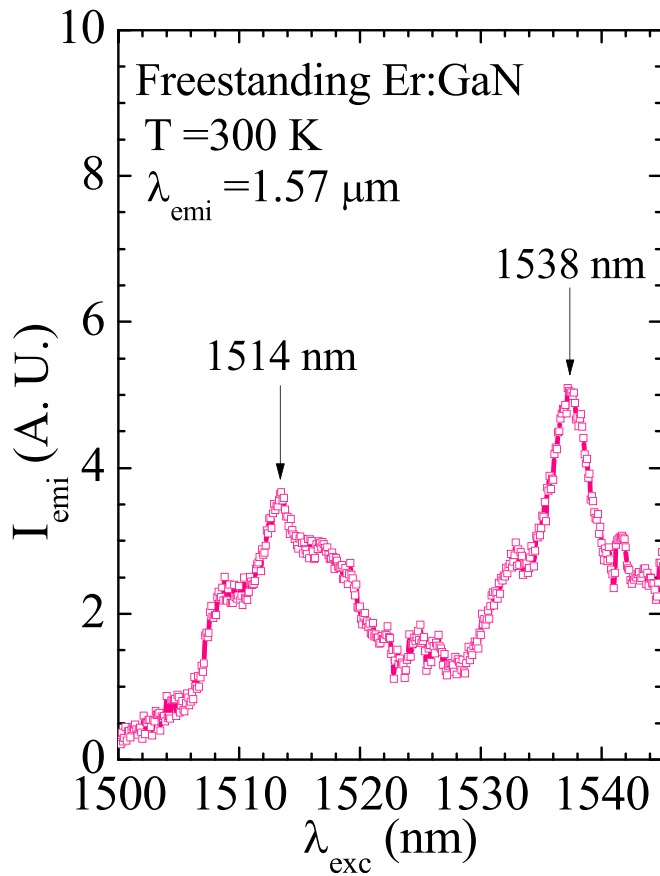


FIG. 3. Room temperature photoluminescence excitation spectrum of a freestanding Er:GaN sample measured at a fixed emission wavelength of $1.57 \mu\text{m}$, with the excitation wavelength scanning from 1500 nm to 1545 nm.

energy band diagrams of Er ions in YAG and glass hosts. As such, the transition between the bottom of the $^4I_{15/2}$ ground state manifold and the top of the $^4I_{13/2}$ first excited state manifold has frequently been thought to be at 1470–1480 nm (Ref. 26) in the past, whereas the present results clearly revealed that the relevant resonant absorption line is in fact appearing at 1514 nm in Er:GaN. It is also interesting to note that for Er:GaN resonantly pumped at $\lambda_{\text{pump}} = 1514$ or 1538 nm and with possible lasing at $\lambda_{\text{laser}} = 1569$ or 1581 nm, the quantum defect, defined as $Q = 1 - \lambda_{\text{pump}}/\lambda_{\text{laser}}$, can be as low as 1.9%–4.2%, which is smaller than that of Er:YAG lasers typically having $Q = 5.1\%$ –10.6%, with $\lambda_{\text{pump}} = 1470$ or 1534 nm, $\lambda_{\text{laser}} = 1617$ or 1645 nm.^{32–35} Lower quantum defects imply less heat generation during a laser operation, which is very desirable for HEL applications.

The measured absorption cross-section of Er in GaN at 1538 nm of about $2.7 \times 10^{-20} \text{ cm}^2$ is larger than those of the corresponding resonant transition lines in YAG ($1.3 \times 10^{-20} \text{ cm}^2$ at 1534 nm)³⁶ as well as in various glass hosts ($\sim 0.6 \times 10^{-20} \text{ cm}^2$ at 1540 nm).³⁷ This relatively large optical absorption cross section measured for Er in GaN further strengthens the view that Er:GaN is a favorable gain medium, as the larger is the cross section the easier it is to achieve amplification and lasing in a gain medium. The absorption cross-sections at 1514 nm and 1538 nm directly measured from freestanding Er:GaN bulk crystals synthesized by HVPE here also match well with the absorption cross-sections at the same wavelengths deduced from an PL

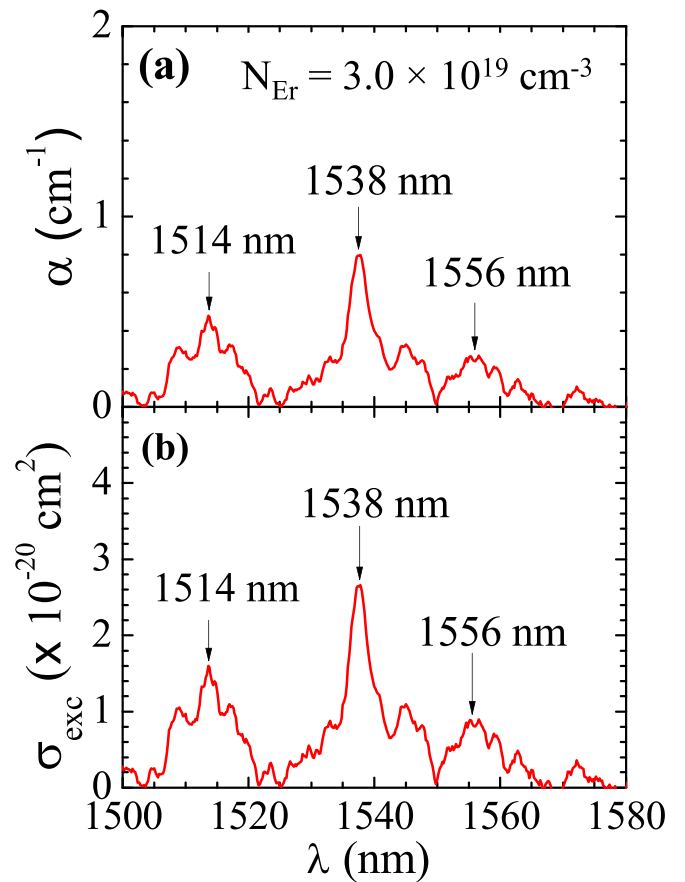


FIG. 4. (a) Absorption coefficients and (b) absorption cross-sections of a freestanding Er:GaN sample (with $N_{\text{Er}} = 3.0 \times 10^{19} \text{ ions/cm}^3$) measured in the $1.5 \mu\text{m}$ window.

emission spectrum together with the use of the McCumber's theory for Er:GaN epilayers prepared by MOCVD,²⁶ despite the fact that there are differences in terms of crystalline qualities, material thicknesses, and Er concentrations between materials produced by HVPE and MOCVD. This is expected since we are dealing with atomic transitions and core electrons excitations of Er in the GaN.

The agreement between the directly measured values here and the values indirectly deduced previously²⁶ for the absorption cross-sections offers high confidence in the measured values as well as a useful guidance to the design of Er:GaN laser gain media. For instance, for a waveguide or slab laser structure having an Er doping concentration of $N_{\text{Er}} = 5 \times 10^{19} \text{ cm}^{-3}$, the absorption coefficient of Er^{3+} at 1538 nm will be $\alpha = 1.35 \text{ cm}^{-1}$. To the first order without taken into consideration of the reflectance at the front and back facets of the waveguide, the optical loss coefficient ($\bar{\alpha}$) must be smaller than the product of the confinement factor (Γ) and gain coefficient (g_{th}) in order to achieve gain, i.e., $\bar{\alpha} < \Gamma \cdot g_{\text{th}} = 1.21 \text{ cm}^{-1}$, if we assume $\Gamma = 90\%$ and $g_{\text{th}} \approx \alpha$.

In summary, we have synthesized freestanding Er:GaN bulk crystals using HVPE technique. The availability of bulk Er:GaN crystals made possible the direct measurements of PL excitation and optical absorption spectroscopy and hence the fundamentally important parameters of the optical absorption cross-sections of Er doped GaN in the technologically significant $1.5 \mu\text{m}$ spectral window. The results established that the optimal pumping wavelengths are 1514 nm and 1538 nm to

achieve low quantum defect Er:GaN lasers. The directly measured optical absorption cross-sections of Er in GaN are $1.42 \times 10^{-20} \text{ cm}^2$ at 1514 nm, $2.70 \times 10^{-20} \text{ cm}^2$ at 1538 nm, and $0.95 \times 10^{-20} \text{ cm}^2$ at 1556 nm, from which the maximum optical loss coefficient for achieving gain has been estimated to serve as the first order guideline for the design of Er:GaN laser and amplifier structures. In addition to a higher thermal conductivity of GaN than YAG, the absorption cross-sections of Er in GaN appear to be larger than those in YAG, further strengthening the view that Er:GaN is a promising gain medium for HELs.

This work was supported by the Directed Energy–Joint Transition Office Multidisciplinary Research Initiative program and ONR (Grant No. N00014-17-1-2531). H. X. Jiang and J. Y. Lin would also like to acknowledge the support of Whitacre Endowed Chairs by the AT&T Foundation.

- ¹Y. Kalisky and O. Kalisky, *Opt. Eng.* **49**, 091003 (2010).
- ²J. A. Zuech, D. J. Lund, and B. E. Stuck, *Health Phys.* **92**, 15 (2007).
- ³J. Bailey, A. Simpson, and D. Crisp, *Publ. Astron. Soc. Pac.* **119**, 228 (2007).
- ⁴Y. X. Fan and R. G. Schlecht, U.S. patent 4,995,046 (Feb. 19 1991).
- ⁵N. Ter-Gabrielyan, V. Fromzel, X. Mu, H. Meissner, and M. Dubinskii, *Opt. Lett.* **38**, 2431 (2013).
- ⁶K. Spariosu, V. Leyva, R. A. Reeder, and M. J. Klotz, *IEEE J. Quantum Electron.* **42**, 182 (2006).
- ⁷J. O. White, *IEEE J. Quantum Electron.* **45**, 1213 (2009).
- ⁸M. Němec, J. Šulc, L. Indra, M. Fibrich, and H. Jelínková, *Laser Phys.* **25**, 015803 (2015).
- ⁹T. Sanamyan, *J. Opt. Soc. Am. B* **33**, D1 (2016).
- ¹⁰D. J. Ottaway, L. Harris, and P. J. Veitch, *Opt. Express* **24**, 15341 (2016).
- ¹¹H. Shibata, Y. Waseda, H. Ohta, K. Kiyomi, K. Shimoyama, K. Fujito, H. Nagaoka, Y. Kagamitani, R. Simura, and T. Fukuda, *Mater. Trans.* **48**, 2782 (2007).
- ¹²R. Hui, Y. Wan, J. Li, S. X. Jin, J. Y. Lin, and H. X. Jiang, *IEEE J. Quantum Electron.* **41**, 100 (2005).
- ¹³D. C. Brown, *IEEE J. Quantum Electron.* **33**, 861 (1997).
- ¹⁴T. Taira, *C. R. Phys.* **8**, 138 (2007).
- ¹⁵P. N. Favennec, H. L'Haridon, M. Salvi, D. Moutonnet, and Y. Le Guillou, *Electron. Lett.* **25**, 718 (1989).
- ¹⁶Z. Y. Sun, J. Li, W. P. Zhao, J. Y. Lin, and H. X. Jiang, *Appl. Phys. Lett.* **109**, 052101 (2016).
- ¹⁷C. Ugolini, N. Nepal, J. Y. Lin, and H. X. Jiang, *Appl. Phys. Lett.* **89**, 151903 (2006).
- ¹⁸J. Heikenfeld, M. Garter, D. S. Lee, R. Birkhahn, and A. J. Steckl, *Appl. Phys. Lett.* **75**, 1189 (1999).
- ¹⁹A. J. Steckl and J. M. Zavada, *MRS Bull.* **24**, 33 (1999).
- ²⁰S. Kim, S. J. Rhee, X. Li, J. J. Coleman, and S. G. Bishop, *Appl. Phys. Lett.* **76**, 2403 (2000).
- ²¹R. Dahal, C. Ugolini, J. Y. Lin, H. X. Jiang, and J. M. Zavada, *Appl. Phys. Lett.* **97**, 141109 (2010).
- ²²V. Dierolf, in *Rare-Earth Doped III-Nitrides for Optoelectronic and Spintronic Applications*, edited by K. O'Donnell and V. Dierolf (Canopus Academic Publishing Ltd and Springer SBM, 2010), Chap. 8.
- ²³A. Braud, in *Rare-Earth Doped III-Nitrides for Optoelectronic and Spintronic Applications*, edited by K. O'Donnell and V. Dierolf (Canopus Academic Publishing Ltd and Springer SBM, 2010), Chap. 9.
- ²⁴R. G. Wilson, R. N. Schwartz, C. R. Abernathy, S. J. Pearton, N. Newman, M. Rubin, T. Fu, and J. M. Zavada, *Appl. Phys. Lett.* **65**, 992 (1994).
- ²⁵D. K. George, M. D. Hawkins, M. McLaren, H. X. Jiang, J. Y. Lin, J. M. Zavada, and N. Q. Vinh, *Appl. Phys. Lett.* **107**, 171105 (2015).
- ²⁶Q. Wang, R. Dahal, I.-W. Feng, J. Y. Lin, H. X. Jiang, and R. Hui, *Appl. Phys. Lett.* **99**, 121106 (2011).
- ²⁷M. Stachowicz, A. Kozanecki, C.-G. Ma, M. G. Brik, J. Y. Lin, H. X. Jiang, and J. M. Zavada, *Opt. Mater.* **37**, 165 (2014).
- ²⁸I. W. Feng, X. K. Cao, J. Li, J. Y. Lin, H. X. Jiang, N. Sawaki, Y. Honda, T. Tanikawa, and J. M. Zavada, *Appl. Phys. Lett.* **98**, 081102 (2011).
- ²⁹K. Motoki, T. Okahisa, S. Nakahata, N. Matsumoto, H. Kimura, H. Kasai, K. Takemoto, K. Uematsu, M. Ueno, Y. Kumagai, A. Koukitu, and H. Seki, *J. Cryst. Growth* **237**, 912 (2002).
- ³⁰E. Desurvire, *Erbium-Doped Fibre Amplifiers: Principles and Applications* (John Wiley & Sons, Hoboken, NJ, 1994).
- ³¹Z. Y. Sun, L. C. Tung, W. P. Zhao, J. Li, J. Y. Lin, and H. X. Jiang, *Appl. Phys. Lett.* **111**, 072109 (2017).
- ³²J. W. Kim, D. Y. Shen, J. K. Sahu, and W. A. Clarkson, *Opt. Express* **16**, 5807 (2008).
- ³³L. Zhu, M. J. Wang, J. Zhou, and W. B. Chen, *Opt. Express* **19**, 26810 (2011).
- ³⁴I. Kudryashov and A. Katsnelson, *Proc. SPIE* **7578**, 75781D-1 (2010).
- ³⁵N. W. H. Chang, N. Simakov, D. J. Hosken, J. Munch, D. J. Ottaway, and P. J. Veitch, *Opt. Express* **18**, 13673 (2010).
- ³⁶D. C. Brown, *Laser Phys.* **24**, 085003 (2014).
- ³⁷W. J. Miniscalco, *J. Lightwave Technol.* **9**, 234 (1991).